

MICROSTRUCTURE AND DYNAMIC FRACTURE TOUGHNESS OF POLYPROPYLENE REINFORCED WITH CELLULOSE FIBER

*Craig M. Clemons, USDA Forest Service, Forest Products Laboratory
A. Jeffrey Giacomini, Mechanical Engineering Department, University of Wisconsin
Daniel F. Caulfield, USDA Forest Service, Forest Products Laboratory*

Abstract

The microstructure of injection-molded polypropylene reinforced with cellulose fiber was investigated. Scanning electron microscopy of the fracture surfaces and X-ray diffraction were used to investigate fiber orientation. The polypropylene matrix was removed by solvent extraction, and the lengths of the residual fibers were optically determined. Fiber lengths were reduced by one-half when compounded in a high-intensity thermokinetic mixer and then injection molded. At low fiber contents, there is little fiber orientation; at high fiber contents, a layered structure arises. To better understand mechanisms of fracture under impact loading, dynamic fracture analysis was performed based on linear elastic fracture mechanics. Dynamic critical energy release rates and dynamic critical stress intensity factors were deduced from instrumented Charpy impact test measurements. Dynamic fracture toughness increased with cellulose content and with increasing orientation of fibers perpendicular to the crack direction. A preliminary evaluation of a simple model relating the microstructure to the dynamic fracture toughness shows promise, but further work is needed to assess its validity.

Introduction

Recently, natural fibers have been used as fillers and reinforcements in low-melting-point thermoplastics. When added to thermoplastics, natural fibers represent low-cost, renewable reinforcements that enhance mechanical properties such as stiffness, strength, and heat deflection under load. Having low densities compared with conventional inorganic fillers and reinforcements, these fibers are often used in automotive and packaging applications where the relatively low density of the natural fibers is a major advantage.

The limited fracture toughness of natural-fiber-reinforced thermoplastics at high strain rates can prevent their use in some applications. To understand and ultimately improve the fracture performance of these composites, it is necessary to have a thorough understanding of the composite microstructure and how it relates to fracture toughness. Because of methodological difficulties, little work has been performed on

characterizing the microstructural parameters such as fiber length and fiber orientation distributions in natural-fiber-reinforced thermoplastics. Even less work has been done relating microstructure to composite performance. This research was undertaken to explore the effect of microstructure on the dynamic fracture toughness of cellulose-fiber-reinforced polypropylene.

Experimental

Materials

The polypropylene was a 12 melt flow index homopolymer (Fortilene 1602, Solvay Polymers, Inc.). The cellulose fibers were a bleached chemical dissolving pulp fiber supplied as pressed and dried pulp sheets (Ultranier-J, Rayonier).

Composite Preparation

The polypropylene and cellulose fiber were compounded in a 1-L, high-intensity thermokinetic mixer (K Mixer; Synergistics, Inc.). The material was discharged at a set temperature and granulated. Batches of 150 g were processed at a rotor speed of 5,000 rpm (rotor tip speed of 32.9 m/s) with discharge temperatures ranging from 180-210°C depending upon the cellulose fiber loading. Resulting batch times ranged from 30-60 s. It was necessary to vary the processing conditions to insure adequate dispersion and proper discharge.

The compounded material was dried at 105°C for at least 4 h before injection molding. A Cincinnati Milacron 33-ton reciprocating screw injection molding machine (Cincinnati Milacron) was used to mold plaques measuring 76 by 127 by 6.4 mm (3 by 5 by 1/4 in.). Barrel temperatures were kept below 200°C, and the mold temperature was 40°C. Injection speeds and pressures necessarily varied with the different formulations and material viscosities.

Dynamic Fracture Tests

Longitudinal and transverse specimens measuring 63.5 by 12.7 by 6.4 mm (2.5 by 1/2 by 1/4 in.) were cut from the injection-molded composite plaques (Figure 1). These

This article was written by U.S. Government employees on official time, and it is therefore in the public domain and not subject to copyright. The use of trade or firm names is for reader information only and does not imply endorsement by the U.S. Department of Agriculture of any product or service.

were then notched with a fly cutter (V notch, 45° angle) to the desired depth, and the crack was sharpened with a razor blade. Specimens were tested at a speed of 1 m/s on a Dynatup GRC 8250 instrumented impact tester (gravity driven) with related software (GRC Instruments). A Charpy jig with a 51-mm (2-in.) span was used.

Fracture surfaces were sputtered with gold and analyzed on a Jeol JSM-840 Scanning Electron Microscope (SEM) at a working distance of approximately 25 mm and a voltage of 15 kV.

Fiber Orientation Determination

For fiber length and orientation determinations, specimens were divided into five layers of equal thickness yielding two surface, two intermediate, and one core layer.

Surface, intermediate, and core layers of each composite were extracted in xylenes for 8 h. The resulting cellulose fiber mats were analyzed using a Siemens Diffractometer with related software (Siemens Energy and Automation). Each extracted sample was irradiated with Cu K α X-rays for 60 s at 40kV and 20 mA using a 0.8-mm collimator. The resulting intensities from the [200] plane at $2\theta = 22.9^\circ$ were used to determine the orientation parameters using the following equations (1):

$$f_p = 2 \langle \cos^2 \chi \rangle - 1 \quad [1]$$

$$\langle \cos^2 \chi \rangle = \frac{\sum N(\chi_i) \cos^2 \chi_i}{\sum N(\chi_i)} \quad [2]$$

where χ is the azimuthal angle, $N(\chi)$ is the intensity at a given χ . Because there is a distribution of cellulose crystals around the fiber axis, values of $|f_p|$ were artificially low. Instead of attempting to quantitatively deconvolute the fiber orientation and cellulose crystal distributions, an approximate method was used. The orientation parameter f_p was normalized using an average orientation parameter of solid loblolly pine (*Pinus taeda*), which was used to represent a perfectly aligned composite.

Fiber Length Determination

Approximately 0.4 mg of residual fibers from the extracted samples were dispersed in 1 L of deionized water. Fiber lengths were then measured by an optical method in a Kajaani FS-100 measurement apparatus (Kajaani GmbH Automation). The cellulose fibers were forced through a capillary pipette located between a light source and a photocell. The shadow falling on the diodes in the detector provided the information for calculation of fiber length. A minimum of 2,000 fibers were measured for each sample. Average fiber lengths were calculated using

$$L_n = \frac{\sum n_i l_i}{\sum n_i} \quad [3]$$

$$L_m = \frac{\sum n_i l_i^3}{\sum n_i l_i^2} \quad [4]$$

where L_n and L_m are the number and length-square average fiber lengths, respectively, and n is the number of fibers of length l in the i th range. An average fiber diameter D of 20 μm was determined by examining many scanning electron micrographs and was used in determining aspect ratios.

Results and Discussion

Composite Microstructure

SEM micrographs of high-cellulose-fiber-content composite showed a layered structure (shown schematically in Figure 1) similar to that of injection-molded glass-fiber-reinforced thermoplastics described by others (1). As the melt enters the mold, the sudden increase in dimensions of the channel causes a deceleration, resulting in a compressive force along the flow direction. This compression results in an alignment of fibers transverse to the melt flow direction. Fibers near the surface of the plaques become oriented parallel to the filling through elongational flow at the flow front described by Rose as the "fountain effect" (2). Because of rapid injection speeds, flow in the core region is nearly plug flow, and the transverse fiber alignment created at the gate is maintained. This morphology was most obvious in the composite samples with higher fiber contents. Figures 2 and 3 show different regions of a fracture surface of a longitudinal specimen showing this layered structure. Because of difficulties in identifying precise transitions between core and surface morphologies, each sample was divided into five layers of equivalent thickness (one core, two surface, and two intermediate layers) for further microstructural analyses (Figure 1).

Figure 4 summarized the orientation parameters f_p from the X-ray analysis. The f_p function yields a positive value for orientation in the flow direction, a negative value for orientation across the flow direction, and nearly zero for random orientation. The trends shown in Figure 4 confirm observations from the SEM work. Fiber orientation is perpendicular to the flow direction in the core layer and parallel to the flow direction in the surface layer. This layered structure decreases with decreasing cellulose fiber content, and nearly random orientation is found at low cellulose fiber contents.

Number average aspect ratios L_n/D and L_w/L_m ratios are summarized in Table 1. Average aspect ratios were cut in half during compounding and injection molding. Surprisingly, the fiber lengths were approximately the

same for composites containing different fiber contents, despite the differences in viscosities and processing conditions during compounding and molding.

Fracture Toughness Tests and Modeling

Linear elastic fracture analysis (3) was used to evaluate dynamic fracture toughness of whole specimens before sectioning. For evaluation of dynamic critical stress intensity factors $K_{c,c}$, the following equation was used:

$$\sigma Y = K_{c,c} (a)^{-1/2} \quad [5]$$

where σ is the maximum gross bending stress, Y is a calibration factor; and a is crack length. Inertial energy effects were previously determined to be negligible for the experimental setup used (4). Specimens with various crack depths were tested, and fracture toughness parameters were determined from the slopes of σY plotted against $(a)^{-1/2}$. A minimum of 10 specimens were used for each $K_{c,c}$ determination. Values for Y have been determined elsewhere (5).

Figure 5 summarizes the critical stress intensity values. The increase in fracture toughness with fiber content is consistent with reports of other reinforcing fibers in polypropylene (1). Little difference in fracture toughness was seen between transverse and longitudinal specimens. What difference there is can be attributed to the greater overall fiber alignment across the crack path in the transverse specimens (Figures 1 and 4).

Friedrich's microstructural efficiency model has been used to relate microstructure to fracture performance of various short-fiber composites (1,6,7). The following form of Friedrich's model was used in this research:

$$\frac{K_{c,c}}{K_{c,M}} = a^* + nR \quad [6]$$

where $K_{c,c}$ is the fracture toughness of the composite and $K_{c,M}$ is the toughness of the matrix. The factor a^* is the matrix toughness correction factor, which reflects changes in the fracture toughness of the matrix material itself as a result of the presence of the fibers (for example, transcrystallinity at fiber-matrix interfaces). The factor n is the energy absorption ratio and is a measure of the increase in toughness directly attributed to the fibers (fiber debonding, pull-out, or fracture). R is the reinforcement effectiveness factor and is of the form:

$$R = \sum_i T_{rel,i} V_{f,i} F_{L,i} F_{O,i} \quad [7]$$

where $T_{rel,i}$ is the thickness of the i th layer relative to the overall thickness, $V_{f,i}$ is the volume fraction of the i th layer, and $F_{L,i}$ and $F_{O,i}$ are the fiber length and orientation efficiency factors. In this study, the microstructural parameters are summed over the surface, intermediate, and core layers.

Although the thickness and volume fraction are easily represented, efficiency factors for the length and orientation distributions, $F_{L,i}$ and $F_{O,i}$, are more difficult. As a first-order approximation of the aspect ratio distribution, Karger-Kocsis and Friedrich (6) proposed using the product of maximum aspect ratio and a representation of the width of the distribution curve:

$$F_O = \frac{(L/D)_{max} (L/D)_n}{(L/D)_m} \quad [8]$$

where $(L/D)_{max,i}$ is the peak aspect ratio and $(L/D)_{n,i}$ and $(L/D)_{m,i}$ are the number- and length-square average aspect ratios.

The effective orientation parameter, $f_{p,eff,i}$, is given by

$$f_{p,eff} = \alpha [1 + \tanh(\beta f_p)] \quad [9]$$

where f_p is the orientation factor determined by Equations [1] and [2], $\alpha = 0.5$, and $1 < \beta < 5$ for $0 \leq |f_p| \leq 1$ (6).

Table 1 summarizes the microstructural data and calculated reinforcing effectiveness parameters. The reinforcing effectiveness factors were determined for each composite according to Equation [7] and were plotted against a normalized critical stress intensity (Figure 6). An approximate linear correlation was found, with little scatter despite the dynamic nature of the test. Values of 1.19 and 0.33 were found for a^* and n , respectively. The fact that a^* exceeds 1 indicates a slight improvement of the matrix toughness itself with fiber addition. The positive value of n indicates the improvement in fracture toughness of polypropylene with addition of cellulose fiber.

Although good correlation between the fracture toughness and microstructure was found, work to date has not tested several aspects of the model. For example, little change was seen in fiber length distribution, and a considerably larger R value range is desirable. Changing key processing parameters would alter composite morphology and, ultimately, fracture toughness. An investigation of this type would demonstrate how fracture toughness can be controlled through processing and provide a greater test of the proposed model. Future work will address these areas.

Conclusions

1. Number average aspect ratios L_n/D were reduced by one-half when-compounded in a high intensity thermokinetic mixer and then injection molded.
2. At low fiber contents, there was little fiber orientation; at high fiber contents, a layered structure arose.
3. Dynamic fracture toughness increased with cellulose content and with increasing orientation of fibers perpendicular to the crack direction.

A preliminary evaluation of a simple model relating microstructure to dynamic fracture toughness showed promise, but further work is needed to assess its validity over broader fiber length and fiber orientation ranges.

Acknowledgments

The authors gratefully acknowledge Solvay Polymers, Inc., and Rayonier, Inc., for supplying the polypropylene and cellulose fiber. The authors also thank the Chemical Engineering Department of the University of Wisconsin for the use of their X-ray equipment and the National Center for Agricultural Utilization Research for use of their impact testing equipment

References

1. D.E. Spahr, K. Friedrich, J.M. Schultz, and R.S. Bailey, *Journal of Materials Science*, **25**:4427–4439, 1990
2. W. Rose, *Nature* **191**:242, 1961
3. E. Plati and J.G. Williams, *Polymer Engineering and Science*, **15**(6):470–477, 1975
4. C.M. Clemons, A.J. Giacomini, and D.F. Caulfield, *Polymer Engineering and Science*, June 1997, **37**(6):1012–1018, 1997
5. K. Friedrich, ed., *Application of Fracture Mechanics to Composite Materials*, Elsevier Science Publishers B.V., New York, NY, 189–248, 1989
6. J. Karger-Kocsis and K. Friedrich, *Composites Science and Technology*, **32**:293–325, 1988
7. K. Friedrich, *Composites Science and Technology*, **22**:43–74, 1985

Keywords: Fracture toughness, microstructure, fiber orientation, cellulose fiber

Table 1: Summary of microstructural data for cellulose fiber and cellulose fiber/polypropylene composites^a

CF (wt. %)	Layer ^b	Volume fraction V_f	Fiber orientation parameter ^c f_p	Effective fiber orientation parameter $f_{p,eff}$	Aspect ratio L_n/D	L_n/L_m	Reinforcement effectiveness factor ^d		
							R_L	R_T	
Fiber									
100	NA	NA	NA	NA	51.0	0.38	NA	NA	
Composites									
10	C	0.067	-0.03	0.43	23.0	0.29			
	I	0.067	-0.04	0.40	23.0	0.30	0.19 ^e	0.23	
	S	0.059	0.04	0.60	21.5	0.28			
20	C	0.145	-0.49	0.05	21.5	0.29			
	I	0.145	-0.14	0.22	22.5	0.31	0.31	0.68	
	S	0.140	0.25	0.89	23.0	0.34			
30	C	0.240	-0.80	0.05	24.0	0.29			
	I	0.210	-0.17	0.19	23.5	0.30	0.45	1.07	
	S	0.208	0.29	0.90	23.0	0.31			
40	C	0.339	-0.85	0.06	24.5	0.29			
	I	0.316	-0.35	0.07	24.0	0.29	0.60	1.66	
	S	0.311	0.52	0.95	23.0	0.32			

^a CF, cellulose fiber; NA, not applicable.

^b C, center layer; I, intermediate layer; S, surface layer.

^c Orientation parameters calculated using flow direction as reference direction.

^d For calculation of R values, $f_{p,eff}$ used for transverse specimens, $1 - f_{p,eff}$ for longitudinal specimens. R values refer to the summation of the C, I, and S layers and are calculated using Equation [7].

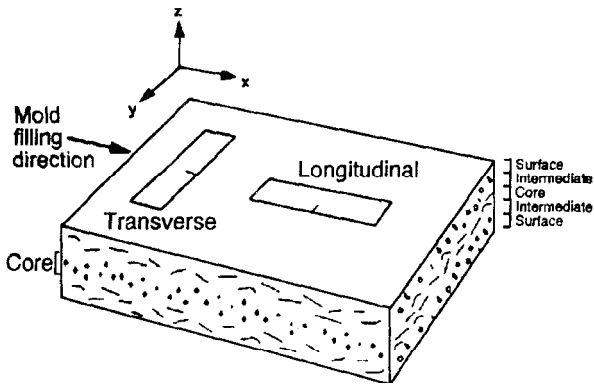


Figure 1. Fiber alignment with respect to melt flow direction for high fiber content composites. Longitudinal and transverse specimen orientation is also shown.

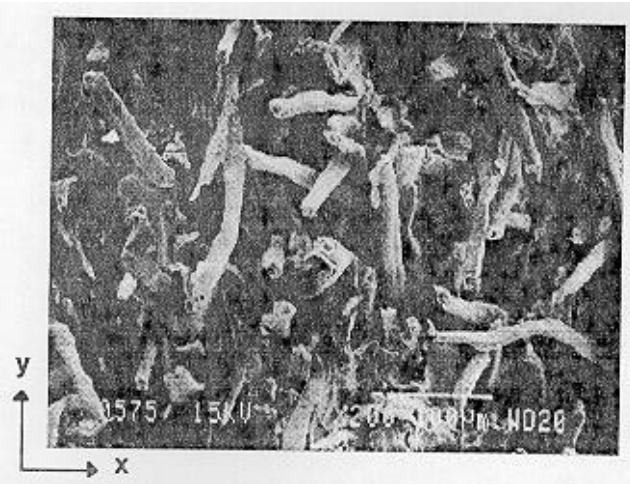


Figure 2. Fracture surface of 40% cellulose fiber composite near outer surface of a longitudinal specimen. Fiber orientation out of y-z plane (reference figure 1).

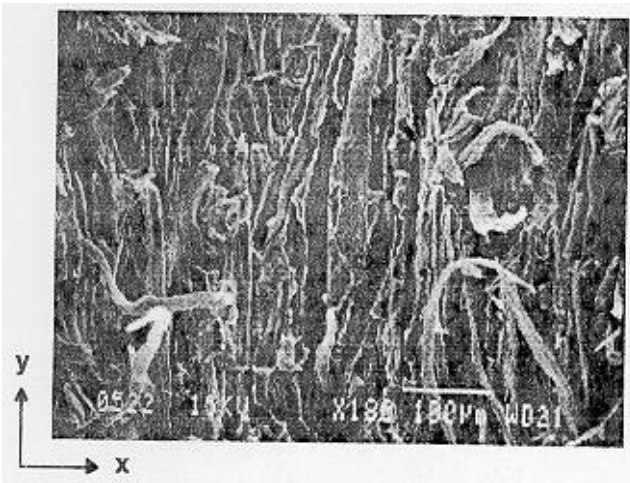


Figure 3. Fracture surface of 40% cellulose fiber composite at the core of a longitudinal specimen. Fiber orientation in the y direction of the y-z plane (reference figure 1).

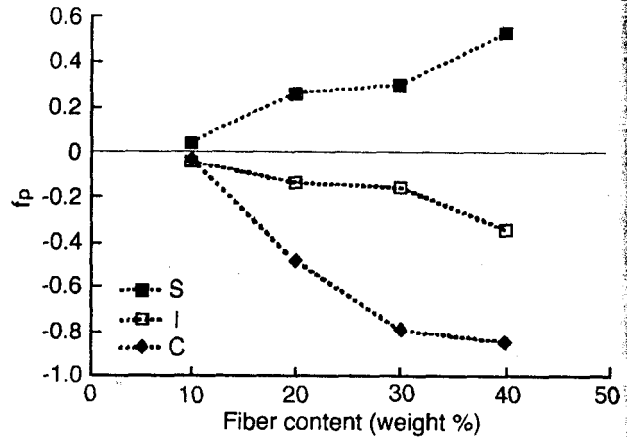


Figure 4. Results of fiber orientation parameter determinations. (S, surface; I, intermediate; C, core.)

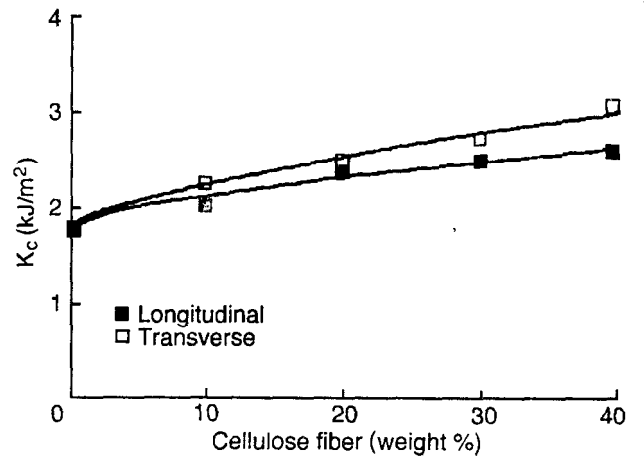


Figure 5. Effect of fiber content on dynamic critical stress intensity factors (K_c). Longitudinal and tangential specimens.

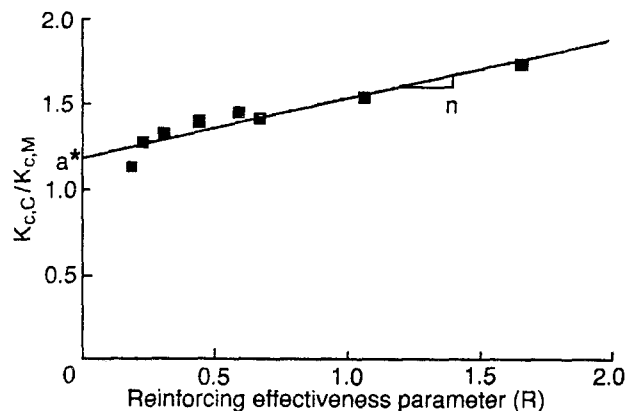


Figure 6. Effect of microstructure on dynamic fracture toughness. $K_{c,C}/K_{c,M}$ is the ratio of fracture toughness of the composite to fracture toughness of the matrix.